esa

ECOSPHERE

Total belowground carbon flux in subalpine forests is related to leaf area index, soil nitrogen, and tree height

E. Berryman,[1,]† M. G. Ryan,[2,3] J. B. Bradford,[4] T. J. Hawbaker,[1] and R. Birdsey[5]

[1]*U.S. Geological Survey Geosciences and Environmental Change Science Center, Denver, Colorado 80225 USA*
[2]*Natural Resources Ecology Laboratory, Colorado State University, Fort Collins, Colorado 80523 USA*
[3]*USDA Forest Service, Rocky Mountain Research Station, Fort Collins, Colorado 80521 USA*
[4]*U.S. Geological Survey Southwest Biological Science Center, Flagstaff, Arizona 86011 USA*
[5]*US Forest Service Northern Research Station, Newtown Square, Pennsylvania 19073 USA*

Citation: Berryman, E., M. G. Ryan, J. B. Bradford, T. J. Hawbaker, and R. Birdsey. 2016. Total belowground carbon flux in subalpine forests is related to leaf area index, soil nitrogen, and tree height. Ecosphere 7(8):e01418. 10.1002/ecs2.1418

Abstract. In forests, total belowground carbon (C) flux (TBCF) is a large component of the C budget and represents a critical pathway for delivery of plant C to soil. Reducing uncertainty around regional estimates of forest C cycling may be aided by incorporating knowledge of controls over soil respiration and TBCF. Photosynthesis, and presumably TBCF, declines with advancing tree size and age, and photosynthesis increases yet C partitioning to TBCF decreases in response to high soil fertility. We hypothesized that these causal relationships would result in predictable patterns of TBCF, and partitioning of C to TBCF, with natural variability in leaf area index (LAI), soil nitrogen (N), and tree height in subalpine forests in the Rocky Mountains, USA. Using three consecutive years of soil respiration data collected from 22 0.38-ha locations across three 1-km^2 subalpine forested landscapes, we tested three hypotheses: (1) annual soil respiration and TBCF will show a hump-shaped relationship with LAI; (2) variability in TBCF unexplained by LAI will be related to soil nitrogen (N); and (3) partitioning of C to TBCF (relative to woody growth) will decline with increasing soil N and tree height. We found partial support for Hypothesis 1 and full support for Hypotheses 2 and 3. TBCF, but not soil respiration, was explained by LAI and soil N patterns ($r^2 = 0.49$), and the ratio of annual TBCF to TBCF plus aboveground net primary productivity (ANPP) was related to soil N and tree height ($r^2 = 0.72$). Thus, forest C partitioning to TBCF can vary even within the same forest type and region, and approaches that assume a constant fraction of TBCF relative to ANPP may be missing some of this variability. These relationships can aid with estimates of forest soil respiration and TBCF across landscapes, using spatially explicit forest data such as national inventories or remotely sensed data products.

Key words: carbon dioxide; carbon sequestration; respiration; soil respiration.

Received 3 March 2016; revised 21 April 2016; accepted 26 April 2016. Corresponding Editor: Y. Pan.

† **E-mail:** eberryman@usgs.gov

Introduction

Forests absorb large amounts of atmospheric carbon dioxide (CO_2) in photosynthesis, but there is considerable uncertainty around regional estimates of the balance between photosynthesis and ecosystem respiration, which determines the net storage rate of C (King et al. 2015). Advances in remote sensing have allowed gross primary productivity or ecosystem photosynthesis (GPP) to be reasonably estimated across large regions (Running et al. 2004). Yet, it remains difficult to characterize ecosystem respiration over large regions because respiration is driven by a complex suite of interacting biological processes and abiotic forcings.

Up to 80% of ecosystem respiration is derived from CO_2 generated in the soil and root zone (Davidson et al. 2006). Forest soil respiration is mostly determined by total belowground C flux (TBCF), the annual flux of C that trees send belowground to fuel root and mycorrhizae growth and respiration and root exudation. A simple C budget technique to quantify TBCF can be readily applied using field measurements of soil C inputs and outputs, that is, soil respiration and litterfall (Raich and Nadelhoffer 1989, Giardina and Ryan 2002). Because landscape-scale measurements of soil respiration and litterfall are laborious and expensive, TBCF estimates across large regions are difficult. Point measurements of TBCF may be scalable across larger landscapes if there are predictable relationships between TBCF and forest properties more readily measured across large regions. Such relationships would better constrain estimates of forest C balance across broad spatial scales. In addition, if TBCF were combined with the measurements of net primary productivity (NPP), rules for forest C allocation may emerge that can be used to test and refine ecosystem process models.

Stand-level manipulative experiments have identified relationships between TBCF and several key properties of forests and soils. Total belowground C flux increases with tree growth and leaf area index (LAI) in young forests, but tends to decrease over time as forests age (Giardina and Ryan 2002, Ryan et al. 2004, Palmroth et al. 2006). Because TBCF is coupled to GPP (Litton et al. 2007), reduced GPP in older, taller trees may be driving the TBCF decline with advancing age (Drake et al. 2010). Further reduction in TBCF at high LAI might also occur because of more active aboveground growth sinks with forest age and increasing LAI (McCarthy et al. 2006, Palmroth et al. 2006). Boosting the supply of belowground resources via fertilization increases GPP but decreases the partitioning of GPP away from TBCF in favor of aboveground NPP (ANPP) (Keith et al. 1997, Ryan et al. 2004, Giardina et al. 2005, Stape et al. 2008). Less clear is whether the annual flux of GPP to TBCF is reduced under high fertility; this effect may be obscured by higher GPP, which would increase overall TBCF (Raich 1998, Giardina and Ryan 2002, Litton et al. 2007). Planting at a high density can increase TBCF via elevated LAI, but partitioning to TBCF may not be altered by density (Giardina and Ryan 2002, Litton et al. 2004). Shifts in TBCF partitioning due to increasing tree height or forest age (Smith and Resh 1999) are unresolved, but the expected response would be that a reduction in photosynthesis in taller trees leads to a decreased demand for belowground resources and reduces the partitioning of C to TBCF (Drake et al. 2010). These stand-level experiments suggest that TBCF is tied to forest GPP, and partitioning of TBCF relative to aboveground components is driven by the supply of soil nitrogen (N) relative to canopy demand. If this is the case, soil respiration surveys and litterfall measurements could be combined with spatially explicit forest structure and soil products to aid with scaling C budgets across forested landscapes that exceed the typical plot size (~400 m^2) of these controlled experiments.

The relationships described above have not yet been examined over highly variable larger landscapes, so we ask: Do observed TBCF patterns in forested landscapes logically reflect mechanistic understanding derived from controlled experiments? If they do, this increases confidence for the use of model-data syntheses to generate regional forest C cycle budgets and predictions. If not, future efforts may need to prioritize refinement of tree and soil physiological mechanisms in ecosystem models, including identification of processes that may be currently unknown or not represented.

Particularly useful would be relationships that allow estimation of belowground carbon flux rates from forest properties that are measured at regional and national scales. For example, the US Forest Service maintains an extensive database of overstory species composition, density, and basal area that is used to estimate regional and national forest C stocks (Forest Inventory and Analysis Program: Bechtold and Patterson 2005) and annual fluxes (Woodbury et al. 2007, Heath et al. 2011). Remote sensing also provides methods to monitor leaf area and time since last disturbance at large spatial scales (Myneni et al. 2002, Duursma et al. 2003, Huang et al. 2010). Finally, soil properties (nitrogen, moisture) may further constrain landscape estimates of TBCF patterns and some of these soil properties can be retrieved from national soil surveys (STATSGO and SSURGO data; Soil Survey Staff, NRCS; http://sdmdataaccess.nrcs.usda.gov/) or

measured with remote sensing (Entekhabi et al. 2010). To detect relationships between TBCF and other forest properties at large spatial scales, sampling should be conducted without bias, with systematic or random sample plot locations and consistent methods used across all sample plots.

The southern Rocky Mountains ecoregion contains extensive areas of subalpine forest, much of which is nitrogen (N) limited (Rollins 2009). Natural and anthropogenic disturbances such as insect outbreaks, wildfires, logging, and N deposition have created heterogeneity in age, structure, and soil fertility in these forests. The results of previous experiments (Giardina and Ryan 2002, Litton et al. 2004, Ryan et al. 2004, and Palmroth et al. 2006) suggest that this variability has created a mosaic of absolute TBCF and partitioning of C to TBCF vs. ANPP across the landscape. We took advantage of this variability and developed a natural experiment that tested three hypotheses:

1. Annual soil respiration and TBCF will show a hump-shaped relationship with leaf area index, with an increase during canopy development and a decline as GPP declines with advancing tree height.
2. Variability in TBCF not explained by LAI will be related to soil N, a proxy for soil N availability, because higher soil fertility increases GPP while decreasing the fraction of GPP used for TBCF.
3. The ratio of TBCF to woody ANPP will decline as soil N or tree height increases, because higher soil fertility decreases the fraction of GPP used for TBCF and photosynthesis decreases with increasing tree height.

Methods

Study site

We studied three subalpine forest sites in the Southern Rocky Mountains, USA, described in Bradford et al. (2008) (Fig. 1). The Fraser and Niwot sites have an overstory species composition of lodgepole pine (*Pinus contorta* Douglas ex Loudon var. *latifolia* Engelm. ex S. Watson), subalpine fir (*Abies lasiocarpa* [Hook.] Nutt.), and Engelmann spruce (*Picea engelmannii* Parry ex Engelm.), with an understory shrub community dominated by *Vaccinium* spp. The Glacier Lakes Ecosystem Experiments Site (GLEES) has a similar species composition, except it lacks lodgepole pine. Total wet N deposition decreases with distance from the major metropolitan area of Denver and is lower on the west side of the Continental Divide than on the east side. This pattern results in high chronic N deposition at Niwot (7.1 $kg{\cdot}N{\cdot}ha^{-1}$) and low N deposition at GLEES and Fraser (2.5 $kg{\cdot}N{\cdot}ha^{-1}$ each; Argerich et al. 2013, National Atmospheric Deposition Program [NADP] 2015).

Measurements

We measured forest C pools and fluxes at nine clusters of four plots systematically located on a grid within 1 km^2 at each of the three study sites (described in Bradford et al. 2010). Cluster size and plot arrangement matched that of the US Forest Service Forest Inventory and Analysis (FIA) program (Bechtold and Patterson 2005). At each plot, species and diameter at breast height (dbh, in cm) was recorded for all live trees with a diameter > 10 cm within an 8 m radius plot. Tree height (in m) was measured from a subset of four to six trees per plot and was predicted for the remaining trees using dbh–height relationships. Understory biomass was measured in three 0.25-m^2 circular plots located 7 m from center at 60°, 180°, and 300°. Species-specific allometric equations were used to determine leaf area from dbh and woody biomass from dbh and height (Table 1). Leaf area from understory was minor in most plots, but because it dominated total leaf area in alpine and wetland plots, we estimated understory leaf area by dividing understory leaf mass by an average leaf mass per projected area of 80 g/m^2 obtained from the literature for subalpine species (Ryan 1995, Ma et al. 2010). Soil C and N stocks were determined from soil samples collected from three locations (located at 60°, 180°, and 300°, 7 m from plot center) within each plot from 0 to 10 cm below the mineral soil surface. Annual litterfall C flux was determined from five 0.15-m^2 litter traps per plot (one at plot center and one each 7 m from the center at 45°, 135°, 225°, 315°), collected once in the spring and fall of 2004–2006. Soil and litter C and N concentrations were measured using a CHN combustion analyzer (LECO, St. Joseph, Michigan, USA). Average stem growth (woody aboveground net primary productivity, or wANPP) from 1994

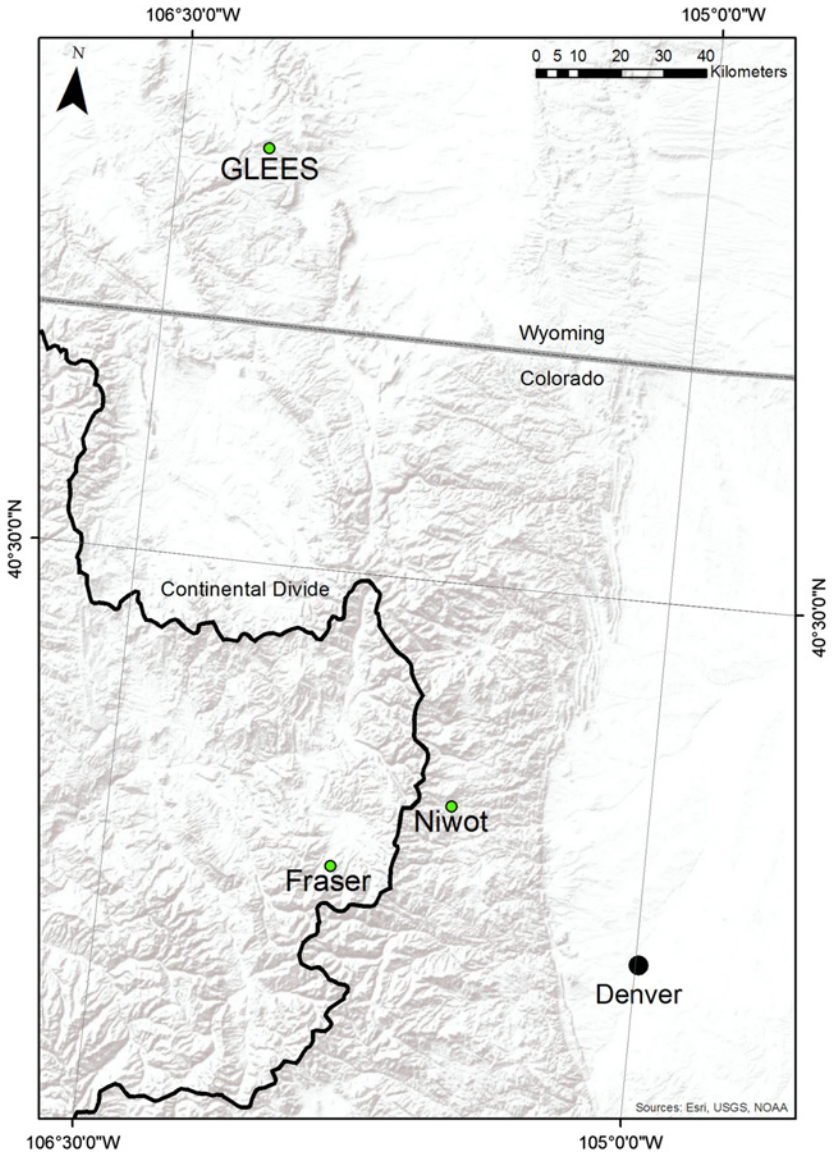

Fig. 1. Location of field sites relative to Denver, Colorado, the Continental Divide, and Front Range of the southern Rocky Mountains.

through 2003 was determined from radial growth measured on increment cores taken from 5 to 10 trees in each plot (reported in Bradford et al. 2008, 2010).

Soil respiration was measured from 2004 to 2006 at these plots and was used only at GLEES for comparison with eddy covariance estimates of ecosystem respiration (Speckman et al. 2015); cluster-level data at GLEES and the other two sites have not yet been published. Soil respiration was measured at three PVC collars (25 cm internal diameter, permanently inserted about 3 cm into the soil in each plot) positioned at 0°, 120°, and 240° and 7 m from plot center at approximate monthly intervals during the snow-free season from 2004 to 2006 using a dynamic closed chamber (Speckman et al. 2015). At the time of respiration measurement, soil temperature was measured at 10-cm depth using a Penetration Probe (Omega Engineering, Stamford, Connecticut, USA) and soil moisture was measured at 12-cm depth in three different places near the collar

Table 1. Equations used to convert tree diameter at breast height (dbh, cm), tree basal area (BA, cm^2), and tree height (HT, m) to leaf area, stem biomass, and coarse root biomass.

Tree species	Leaf area	Stem biomass	Root biomass
Lodgepole pine	[a]$0.0331 \times BA$	[b]$(4.00 \times 10^{-5} \times dbh^2 \times HT + 7.92 \times 10^{-4}) \times 360$	[e]$4.77 + 5.56 \times 0.001 \times \pi\,(dbh/2)^2 \times HT - 1.96 \times 1 \times 10^{-8} \times (\pi\,(dbh/2)^2)^2 \times HT$
Engelmann spruce	[a]$0.0958 \times BA$	[c]$(3.44 \times 10^{-5} \times dbh^2 \times HT + 1.82 \times 10^{-3}) \times 310$	[f]$0.001 \times (421 + 0.0362 \times dbh^2 \times HT \times 100)$
Subalpine fir	[a]$0.0867 \times BA$		
Aspen	[a]$0.0535 \times BA - 0.0000251 \times BA^2$	[d]$0.003 \times dbh^{3.033}$	[gh]$2.00 \times (stem + 0.001 \times dbh^{3.161} + 0.004 \times dbh^{2.143}) \times dbh^{-0.6178}$

Notes: References are indicated with superscript letters: a, Kaufmann et al. (1982); b, Myers (1964); c, Myers (1972); d, Wang et al. (1995); e, Comeau and Kimmins (1989); f, Ker and Raalte (1981); g, Ruark and Bockheim (1988); h, Bond-Lamberty et al. (2002) for saplings and seedlings. Leaf area was summed for each plot and divided by plot area to calculate plot leaf area index (LAI).

(HydroSense; Campbell Scientific, Logan, Utah, USA). Twice during each winter, soil respiration was measured assuming steady-state diffusion into the atmosphere with CO_2 concentration measurements below and above the snowpack at five locations per plot (EGM-4; PP Systems International, Amesbury, Massachusetts, USA) and snow depth and density (Snowmetrics, Fort Collins, Colorado, USA) as described in Massman (1998) and Hubbard et al. (2005).

TBCF calculations

Point measurements of soil respiration were converted into annual values for the period 2004 through 2006 using the following approach. Measurements from the three collars/plot were averaged for each plot and date. Plot-level means were interpolated over a year, combining data from all years. A local regression was fit explaining each plot's respiration trend over day of water year (*loess* using R statistical package [R Development Core Team 2015]), and the area under the curve was calculated to determine the average annual cumulative C respired from 2004 to 2006 for each plot. From annual soil respiration values, annual TBCF was calculated as the difference between annual soil respiration and litterfall C plus increase in storage at the plot level (i.e., C in roots, soil carbon, litter layer C) (Raich and Nadelhoffer 1989, Giardina and Ryan 2002, Giardina et al. 2014). Annual changes in storage of soil C and litter layer C are assumed to be negligible, due to average accumulation rates of < 0.1 $Mg{\cdot}C{\cdot}ha^{-1}{\cdot}yr^{-1}$ (or 1–2% of annual soil respiration) under afforestation in the United States (Nave et al. 2013). We would expect this to be even less in western subalpine forests due to the overall lower productivity than eastern forests, which dominated Nave et al.'s analysis. Change in storage of fine roots is considered to be negligible given their small biomass relative to TBCF (Giardina and Ryan 2002). However, increases in storage of C in coarse roots may constitute 10% of TBCF or more (Giardina and Ryan 2002). Therefore, we estimated annual increases in coarse root C storage for each site from the slope of a linear regression relating coarse root biomass (as estimated using allometric equations; Table 1) to stand age. This annual increase in coarse root C was added to annual TBCF for each plot; on average, this represented less than 5% of annual TBCF (range of 0.1–20%).

Relative flux of belowground C was estimated by dividing TBCF by TBCF plus wANPP for each forest stand. Foliar ANPP was not considered because leaf litterfall was included in both TBCF and foliar ANPP calculations; regardless, we should expect to see a functional tradeoff in C partitioning between roots and stemwood, not between roots and foliage (Beets and Whitehead 1996, Litton et al. 2007).

Statistical analyses

Plot-level soil respiration ($Mg{\cdot}C{\cdot}ha^{-1}{\cdot}yr^{-1}$), TBCF ($Mg{\cdot}C{\cdot}ha^{-1}{\cdot}yr^{-1}$), the ratio of TBCF to TBCF plus woody ANPP (TBCF/(TBCF + wANPP), unitless), LAI, total soil N, and stand height were aggregated to cluster-level means prior to statistical analyses because we expected the scale of influence of aboveground variables on soil respiration or TBCF to be greater than our plot size of 200 m^2 and closer to the size represented by the clusters (~3800 m^2). Because the focus of the

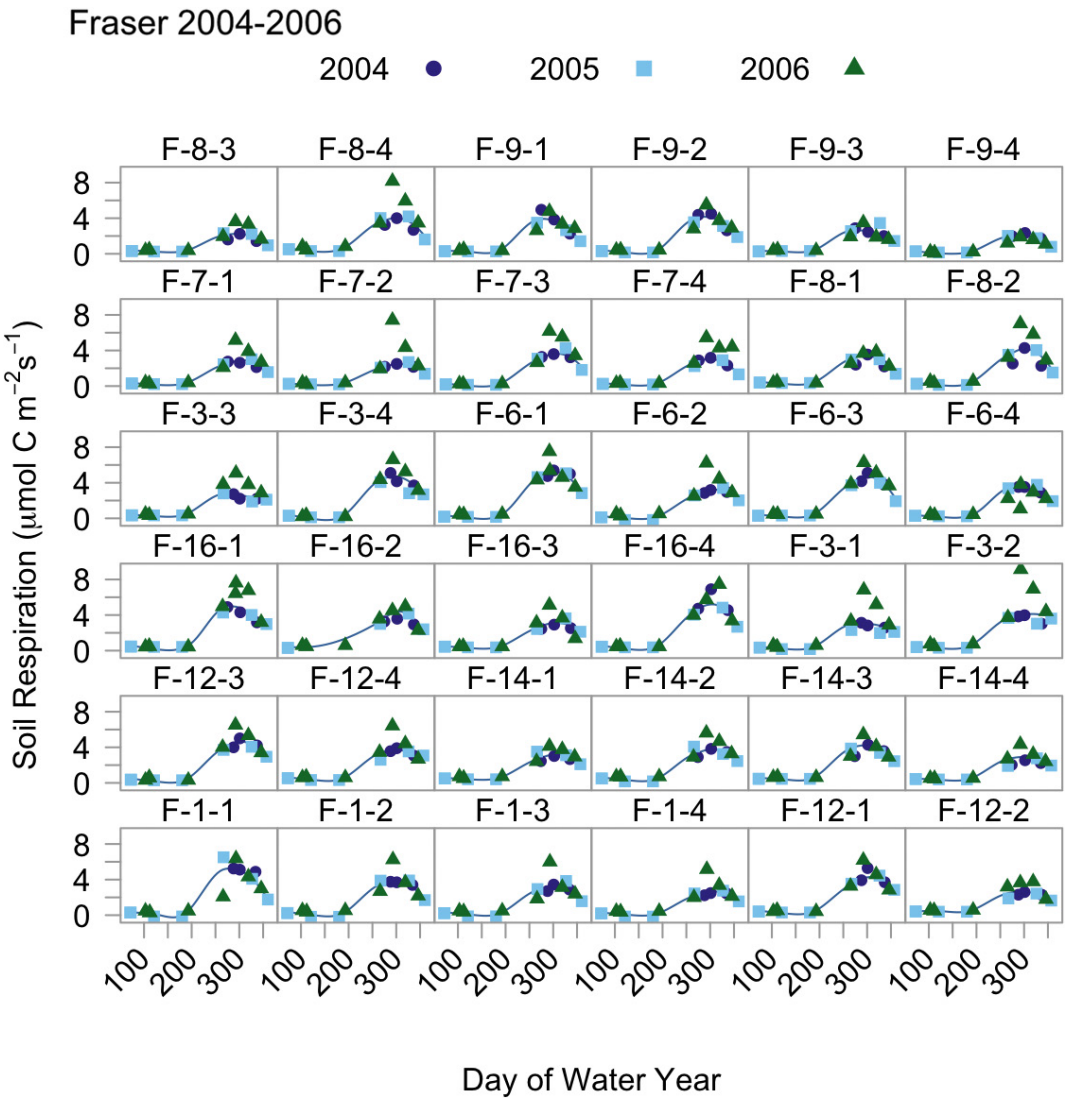

Fig. 2. For the Fraser plots, a spline fit captured the seasonal trend of respiration from 2004 to 2006, with the exception of some high values in 2006. Plot IDs are included at the top of each panel: The first character corresponds to a site, the first set of digits corresponds to a cluster, and the last digit corresponds to a plot within the cluster. Day 1 of the water year corresponds to October 1.

study is conifer forest TBCF, clusters where the center plots fell in aspen stands (*Populus tremuloides* Michx.), alpine meadows, or wetlands were not considered in the statistical analysis, leaving a total of 22 clusters for analysis of the original 27 (all plots in that cluster were omitted because our analytical unit was a cluster-level mean). These clusters were identified by lack of tree basal area and/or high seasonality in the annual normalized difference vegetation index (NDVI) product from Landsat (i.e., deciduousness). TBCF was compared among the three sites using an analysis of variance (ANOVA). Soil respiration ($Mg{\cdot}C{\cdot}ha^{-1}{\cdot}yr^{-1}$), TBCF ($Mg{\cdot}C{\cdot}ha^{-1}{\cdot}yr^{-1}$), and the ratio of TBCF to TBCF plus woody ANPP ("TBCF/(TBCF + wANPP)," unitless) were analyzed for relationships with LAI, total soil N, and stand height. Hypotheses 1 and 2 were tested using ANOVA to compare the fit of a linear second-degree polynomial model between soil respiration or TBCF and LAI and soil N with that of an intercept-only model and a first-degree

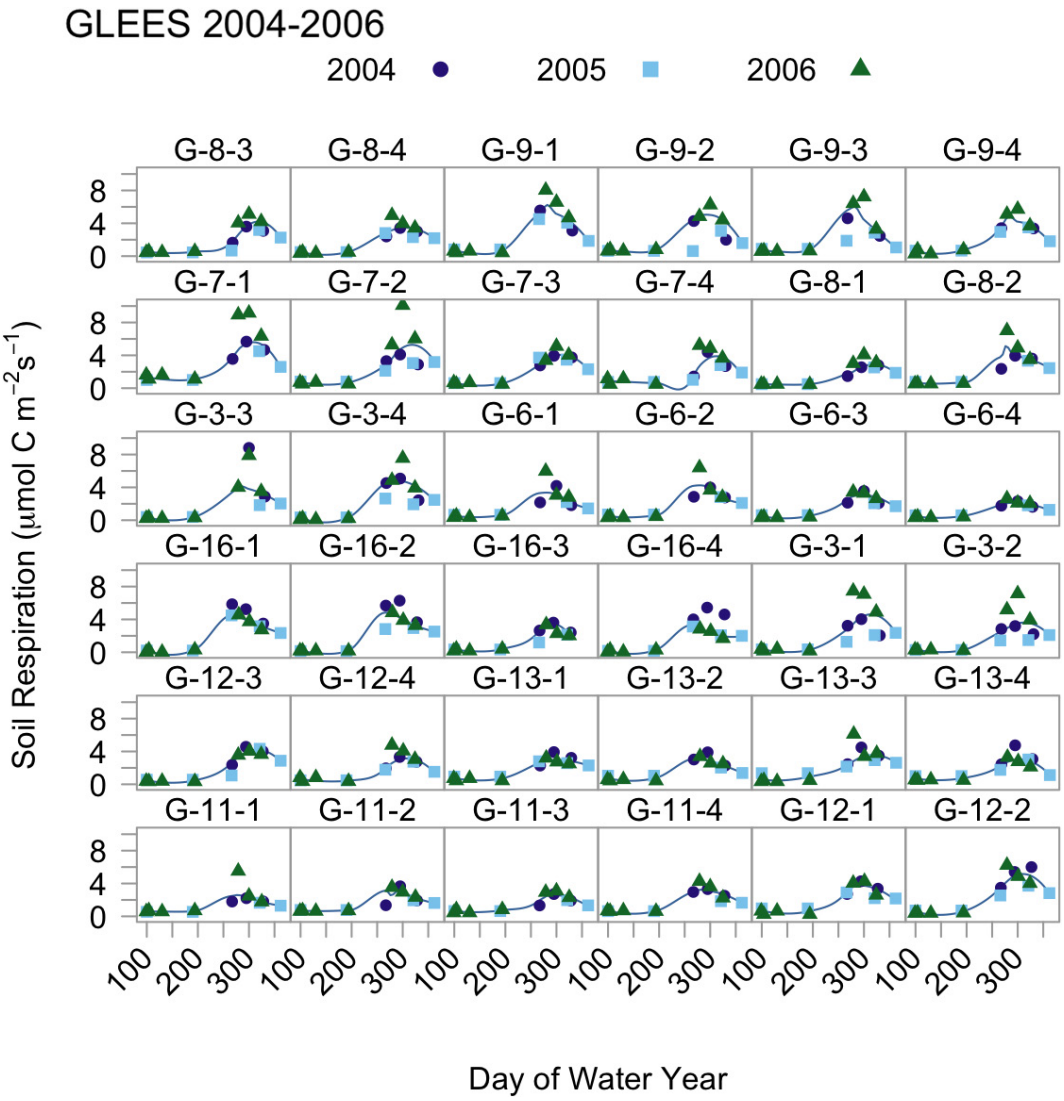

Fig. 3. For the GLEES plots, a spline fit captured the seasonal trend of respiration from 2004 to 2006, with the exception of some high values in 2006. Plot IDs are included at the top of each panel: The first character corresponds to a site, the first set of digits corresponds to a cluster, and the last digit corresponds to a plot within the cluster. Day 1 of the water year corresponds to October 1. Clusters G-7 and G-9 are wetland and clusters G-3 and G-16 are alpine meadow.

linear model fit. Hypothesis 3 was tested similar to the first two hypotheses, by regressing TBCF/(TBCF + wANPP) against total soil N and mean stand height. R software was used for statistical analyses, using the base package for linear model fitting and *t* tests (*lm* and ANOVA functions). Linear model fit was assessed visually based on quantile plots, goodness of fit was assessed using r^2 and *P* values, and prediction uncertainty was assessed using root-mean-squared error (RMSE).

Results

Soil respiration fluxes displayed remarkably consistent seasonal patterns at all three sites from year to year, with the exception of high values in 2006 at a few plots (Figs. 2–4). The mean seasonal peak in respiration was 4.37 µmol·C·m^{-2}·s^{-1} (SD: 1.61) at Fraser, 3.60 µmol·C·m^{-2}·s^{-1} (SD: 1.26) at GLEES, and 4.10 µmol·C·m^{-2}·s^{-1} (SD: 1.01) at Niwot. There was no difference in aggregated

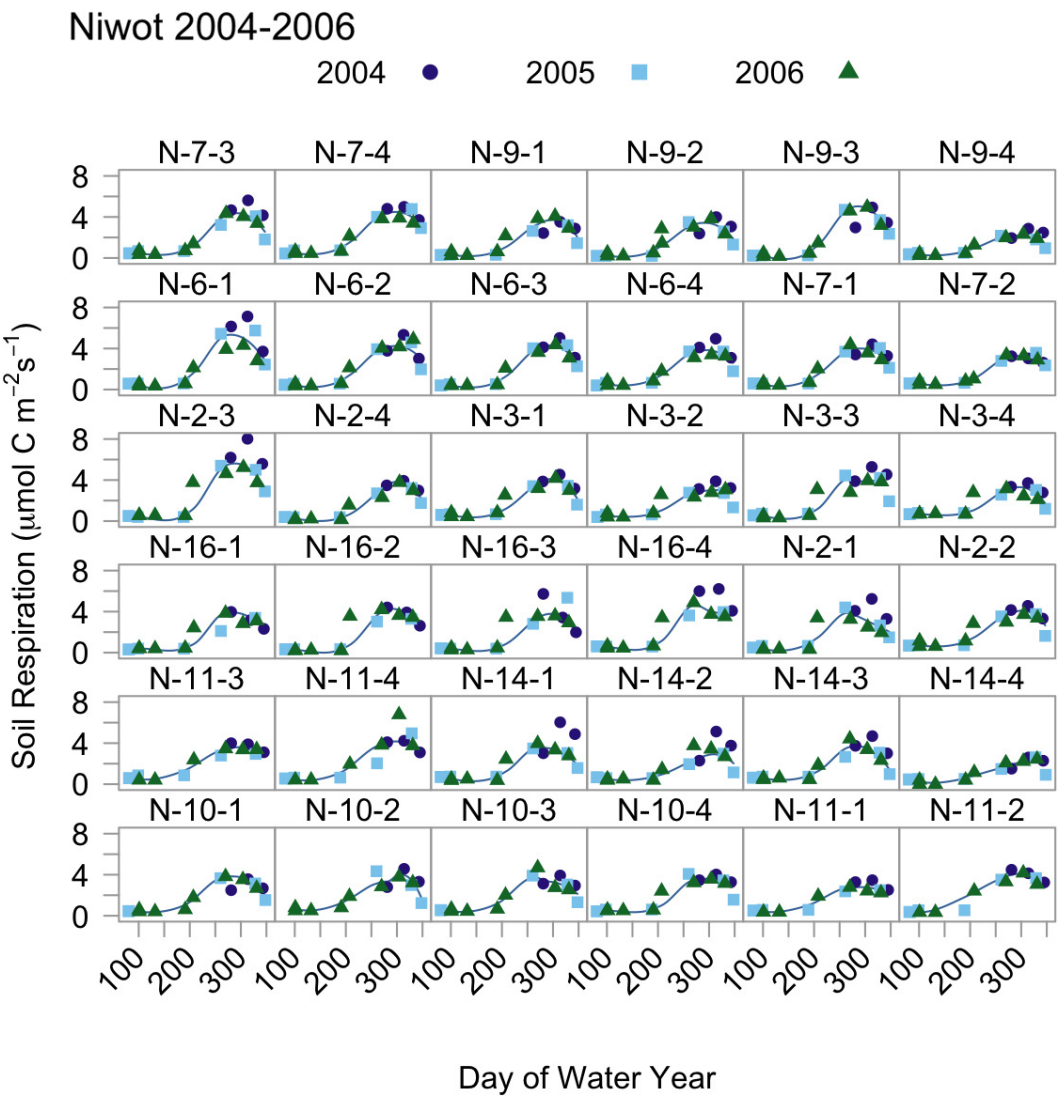

Fig. 4. For the Niwot plots, a spline fit captured the seasonal trend of respiration from 2004 to 2006, with the exception of some high values in 2004. Plot IDs are included at the top of each panel: The first character corresponds to a site, the first set of digits corresponds to a cluster, and the last digit corresponds to a plot within the cluster. Day 1 of the water year corresponds to October 1. Cluster N-16 is located in an aspen clone.

2004–2006 TBCF by site (Fig. 5). Annual cumulative soil respiration was ~4× greater than litterfall and was the major contributor to TBCF, whereas change in coarse root storage was minor (Fig. 5).

Soil respiration showed no significant relationship with LAI (Fig. 6). In contrast, TBCF showed the expected hump-shaped pattern with LAI, as TBCF increased with LAI to about 3.5 m^2/m^2 LAI and then decreased with further increases in LAI (Fig. 7a), supporting our first hypothesis. A polynomial function explained the trend better than both an intercept-only model and a linear model (Table 2; $P < 0.05$). Model RMSE was 0.70 $Mg{\cdot}C{\cdot}ha^{-1}{\cdot}yr^{-1}$, or 14% of the overall mean for TBCF (Table 2). In support of Hypothesis 2, residuals from the TBCF–LAI relationship were related to soil N: A hump-shaped relationship peaked around 2.5·$Mg{\cdot}N{\cdot}ha^{-1}$ (Fig. 7b). Together, LAI and soil N accounted for about half of the variability in TBCF across the three sites (Table 2).

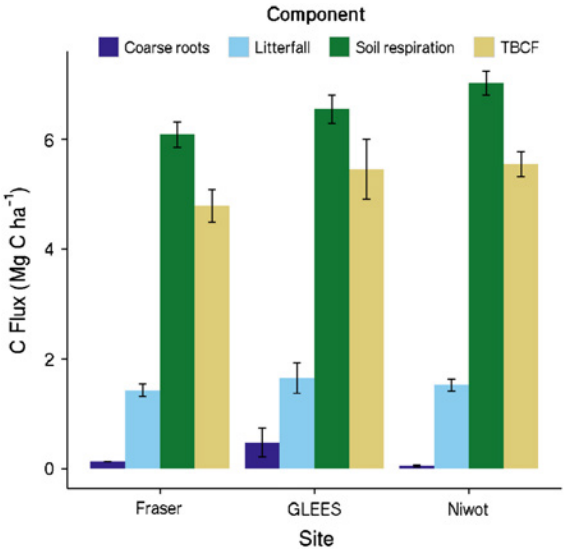

Fig. 5. Total belowground carbon flux (TBCF) and its components: litterfall and soil respiration for each site, averaged from 2004 through 2006. Error bars represent ±1 SE. All clusters are considered in these means (n = 9). An ANOVA found no significant difference in TBCF among the three sites (P = 0.32).

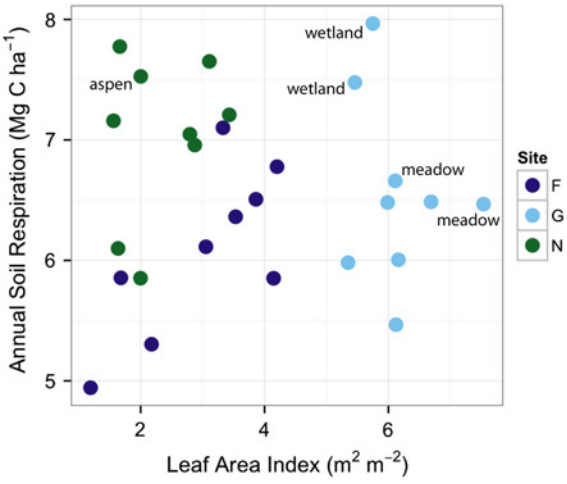

Fig. 6. Average annual soil respiration from 2004 through 2006 was not related to leaf area index. Data from wetland, meadow, and aspen clusters are labeled.

TBCF/(TBCF + wANPP) was negatively related to soil N and mean stand height, in support of Hypothesis 3 (Fig. 8a, b). Together, soil N and mean stand height accounted for 72% of the variability in TBCF/(TBCF + wANPP) (Table 2). There were significant correlations among some of the response variables, which may aid in interpreting landscape patterns. TBCF/(TBCF + wANPP) was correlated to wANPP but not TBCF (Table 3). Both LAI and wANPP were positively correlated to soil N, and stand height, LAI, and stand age were positively correlated (Table 3).

Discussion

TBCF varies with LAI and soil N

We found that total belowground carbon flux had a nonlinear, hump-shaped relationship with leaf area index, in support of the conceptual model proposed by Palmroth et al. (2006). These authors interpreted the relationship between TBCF and LAI as the difference between aboveground net carbon uptake (ANCU, or net photosynthesis minus aboveground woody maintenance respiration) and ANPP′ (ANPP plus construction respiration) trends with LAI, implying a tradeoff between ANPP′ and TBCF. According to this model, TBCF follows ANCU as LAI increases and the canopy closes. After canopy closure, ANCU slows its increase with further LAI increases and lower light capture per unit of LAI, yet demand for C moving into ANPP′ remains high; that is, ANPP′ is not adjusted downward to account for slowing photosynthesis. Instead, trees reduce TBCF to free up additional C to sustain high ANPP′. Net canopy C uptake may be lower than expected at high LAI due to two reasons: (1) High LAI occurs in older and taller trees, and photosynthesis slows in tall trees (Barnard and Ryan 2003, Ryan et al. 2006, Drake et al. 2010), and (2) after canopy closure, light interception approaches saturation and further increases in LAI do little to increase canopy C uptake (Palmroth et al. 2006).

The global positive linear relationship between TBCF and GPP found at all levels of LAI by Litton et al. (2007) in their analysis of many forests worldwide appears at first glance to be inconsistent with our findings and with the Palmroth et al. (2006) hypothesis. However, a closer look suggests that the findings are similar. First, the research summarized in Litton et al. (2007) represents a comparison across sites and species for many different stand ages, where changes in TBCF with forest age in a given species were likely small compared with the variation across sites and species. Second, in Litton et al. (2007),

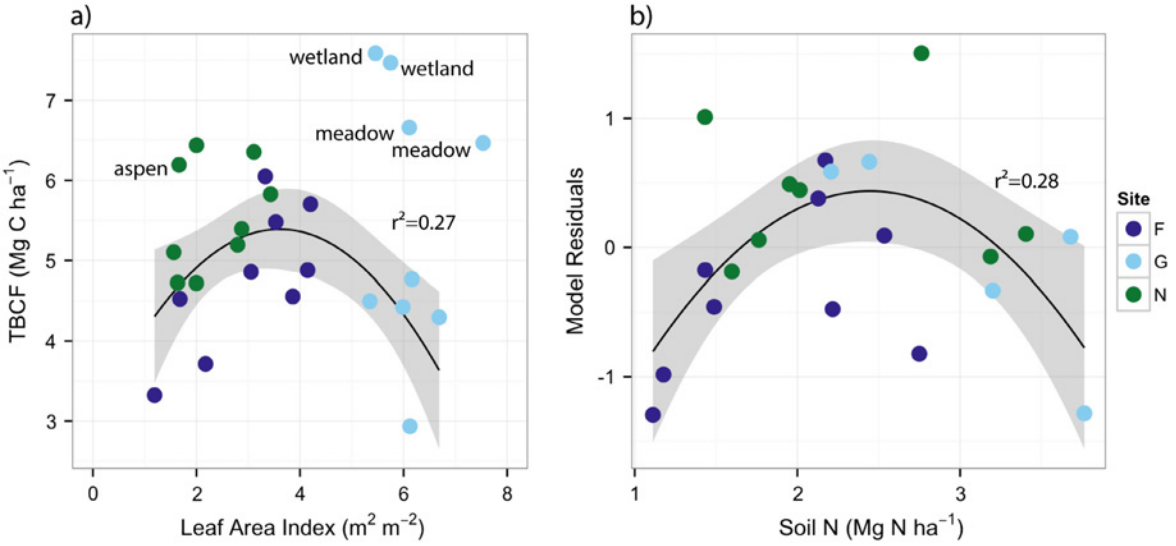

Fig. 7. (a) Total belowground carbon flux (TBCF) shows a peaked relationship with LAI (equation in Table 1). Data from the wetland and aspen clusters are shown, but not included in these or subsequent regressions. TBCF calculated for the meadow plots is equivalent to annual soil respiration because of the lack of trees (i.e., no litterfall or coarse root storage). Residuals from the model are (b) related to total soil nitrogen. Shaded regions represent the 95% confidence interval of the regression.

Table 2. Linear models describing soil respiration and TBCF (in Mg·C·ha^{-1}·yr^{-1}) and TBCF/(TBCF + wANPP) from ecosystem properties.

ANOVA significance	Form	r^2	RMSE	RMSE % of mean
Response variable: Soil respiration				
a	$y = 6.41^{***}$		0.729	11
a	$y = 6.53^{***} - 0.03 \times LAI$	−0.04	0.726	11
a	$y = 5.29^{***} + 0.75 \times LAI - 0.10 \times LAI^2$	0.03	0.682	11
Response variable: TBCF				
	$y = 4.89^{***}$		0.857	18
NS	$y = 5.27^{***} - 0.11 \times LAI$	0.01	0.838	17
*	$y = 2.98^{***} + 1.34 \times LAI^{*} - 0.19 \times LAI^{2**}$	0.27	0.698	14
**	$y = -0.46 + 0.93 \times LAI - 0.14 \times LAI^{2*} + 3.73 \times SoilN^{**} - 0.75 \times SoilN^{2**}$	0.49	0.549	11
Response variable: TBCF/(TBCF + wANPP)				
	$y = 0.84^{***}$		0.053	6
***	$y = 0.94^{***} - 0.05 \times SoilN^{***}$	0.40	0.041	5
*	$y = 1.07^{***} - 0.04 \times SoilN^{**} - 0.01 \times HT^{*}$	0.53	0.035	4
**	$y = -0.09 - 0.02 \times SoilN^{*} + 0.16 \times HT^{**} - 0.01 \times HT^{2**}$	0.72	0.026	3

Notes: An analysis of variance (ANOVA) between models shows that TBCF has a peaked relationship with LAI and soil N and that TBCF/(TBCF + wANPP) declines with both soil N and tree height (HT, in m). TBCF = total belowground carbon flux (Mg·C·ha^{-1}·yr^{-1}), wANPP = woody aboveground net primary productivity, LAI = leaf area index (m^2/m^2), and SoilN = total soil nitrogen (Mg·N·ha^{-1}). Soil respiration units are Mg·C·ha^{-1}·yr^{-1}. The "ANOVA significance" column indicates P values of ANOVA tests of the model comparing it to the simpler model shown one row above. Asterisks indicate significance (*P < 0.05; **P < 0.01; ***P < 0.001). RMSE = root-mean-squared error.

Table 3. Pearson correlations between main variables measured for this study.

Variable	TBCF	TBCF/ (TBCF + wANPP)	LAI (m^2/m^2)	Soil N ($Mg \cdot N \cdot ha^{-1}$)	Height (m)	Age (yr)
wANPP	0.11	−0.85***	0.48*	0.68***	0.26	−0.35
TBCF		0.41	−0.21	−0.05	−0.56**	−0.37
TBCF/ (TBCF + wANPP)			−0.58**	−0.67***	−0.54**	0.15
LAI				0.55**	0.77***	0.32
Soil N					0.34	−0.09
Height						0.63**

Notes: TBCF = total belowground carbon flux, wANPP = woody aboveground net primary productivity, LAI = leaf area index, and Soil N = total soil nitrogen in the top 10 cm. Asterisks indicate significance (*$P < 0.05$; **$P < 0.01$; ***$P < 0.001$).

where data were available for single species with different stand ages, the fraction of GPP used for TBCF decreased for four of five species (Litton et al. 2007: Figure 8; the exception was *Eucalyptus saligna*). Finally, the ratio of TBCF to ANPP decreased as ANPP increased across sites and species (Litton et al. 2007: Figure 5).

Even though LAI was a significant predictor of stand TBCF in this study, our results suggest a considerable variability in this relationship. Some of this variability may be related to soil nitrogen effects on photosynthesis (Binkley et al. 2004), changing TBCF with GPP. Our findings support the hypothesis that further landscape variability in TBCF might be due to spatial changes in total soil N. Elevated soil N may increase TBCF by promoting GPP (Maier et al. 2004), and while we do not have measures of GPP at our plots, NPP showed a positive relationship with soil N (Table 3). However, the decrease in TBCF at levels of soil N above a certain threshold may reflect reduced partitioning of C belowground in response to high N availability (Giardina et al. 2003, Olsson et al. 2005).

TBCF partitioning was related to soil N and tree height

Leaf area index, woody ANPP, and soil N were all positively correlated with each other, suggesting that the highest LAI occurred in the most productive stands growing in the most fertile areas. Despite this rapid gain in C in these trees, TBCF was not the greatest in those stands. We hypothesized that this was due to reduced

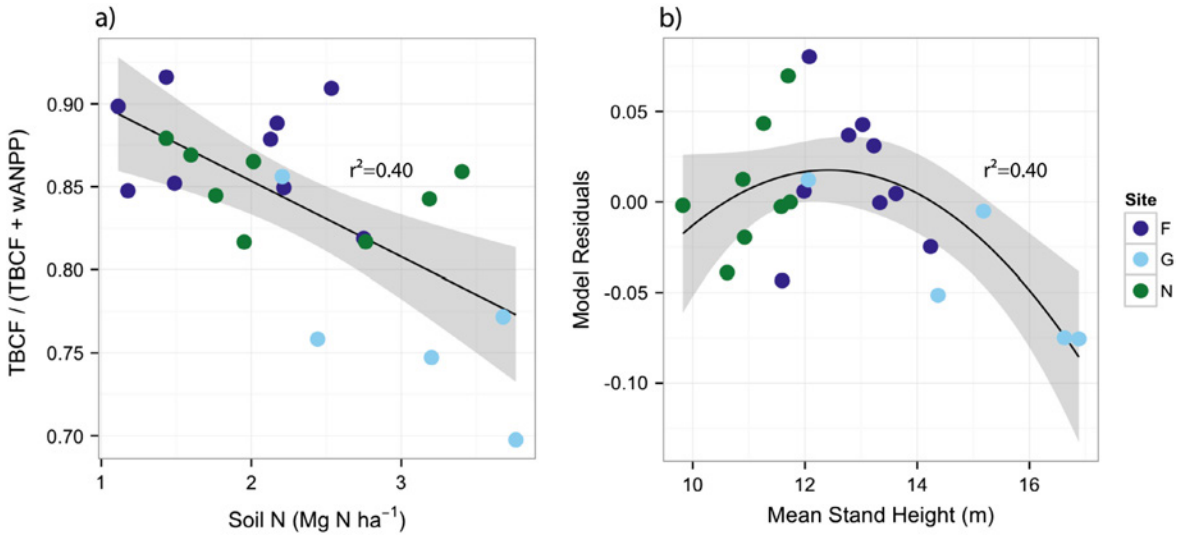

Fig. 8. (a) Flux of C belowground relative to woody ANPP decreased with increasing soil N. Model residuals (b) are related to stand height. Shaded regions represent the 95% confidence interval of the regression.

partitioning of C belowground in response to increased soil N and tree height.

Consistent with this idea, the ratio of TBCF to TBCF plus woody ANPP declined with increasing soil N and tree height. A negative relationship between TBCF or TBCF/(TBCF + wANPP) and soil nutrients has been widely documented in fertilization studies (Keith et al. 1997, Giardina and Ryan 2002, Giardina et al. 2004, Ryan et al. 2004, Forrester et al. 2006). Declining C investment in roots is a predicted outcome of allocation models that optimize tree growth rates or maximize belowground competitive advantage (Franklin et al. 2012). Allocation of C belowground is determined by a balance between the tree's need for additional N (i.e., investment in roots wins out) and the demand for increased aboveground growth (investment in woody growth wins out).

Reduced leaf-level photosynthesis has been measured in tall trees compared with shorter trees and is attributed to hydraulic limitation and reduced stomatal conductance (Ryan and Yoder 1997, Ryan et al. 2006, Ambrose et al. 2009, Drake et al. 2010). This reduction in photosynthesis would relax the demand for soil N to support higher foliage turnover and photosynthesis rates, allowing C to be used to grow aboveground woody tissue instead of supporting fine root production. In support of this hypothesis, we found that after accounting for soil N effects, TBCF/(TBCF + wANPP) was further reduced in the tallest forest stands. Decreased belowground partitioning with increasing stand height may reduce N uptake and could explain increased soil-soluble N availability seen in older, taller forest stands compared with younger stands (Ryan and Waring 1992, Olsson et al. 1997, Smithwick et al. 2009). The humped shape of the relationship suggests the presence of a threshold height around 14–15 m, above which further increases in height result in a rapid decline in TBCF/(TBCF + wANPP). The hump-shaped curve is driven largely by data from Niwot. There, reduced precipitation relative to GLEES and Fraser may have lowered tree height, and the high N deposition may have reduced partitioning to TBCF (see below).

Our findings raise questions about how anthropogenic N deposition may alter the distribution of C within subalpine forests. We found that increases in soil N shift partitioning of new C away from TBCF, an important pathway for creation of new labile soil organic C, and toward the more stable woody pool, thereby increasing the amount of C in long-term storage. High levels of anthropogenic N deposition increase soil N availability and therefore may lead to a decrease in TBCF/(TBCF + wANPP). To look for such an effect in our data, we compared Niwot, the site with high N deposition, to Fraser, the site west of the Continental Divide (Fig. 1) and thus less affected by N deposition yet very similar in terms of climate, tree species, and stand development. Even though soil respiration and TBCF were both higher at Niwot than Fraser, Niwot had significantly lower TBCF/(TBCF + wANPP) than Fraser (t test, $P = 0.045$). High N deposition may reduce TBCF by decreasing allocation to roots (Janssens et al. 2010), or it may have reduced our estimates of TBCF by suppressing organic matter mineralization rates (Berg and Matzner 1997) because soil respiration is the major component of our TBCF calculations. This observation has important implications for global change feedbacks in C cycling, suggesting an increase in woody C sequestration under further increases in N deposition.

Our analysis found that soil respiration and/or TBCF was much higher per unit of LAI in aspen, alpine, and wetland plots than in evergreen forests. Initial data analysis including these data in our models found no significant effect of LAI on TBCF. Visually, these points were outliers (Figs. 6 and 7), and ecologically, we would expect them to function differently than conifer forests. Still, we expect that these systems would also have a relationship between TBCF and LAI. If we had a larger sample size, we could have modeled additional differences due to ecosystem type; however, we did not have enough points in these areas ($n = 1$ aspen, $n = 2$ for meadow, $n = 2$ for wetland) to add ecosystem type as a covariate in our models. If our TBCF–LAI relationships were to be applied to areas containing alpine meadow, aspen, or wetland, the predicted TBCF would likely be an underestimation. Extrapolating our relationships to other subalpine landscapes should consider the contribution of aspen, meadow, or wetland to overall landscape C flux.

Implications for C cycle modeling and landscape estimates

Our findings may aid with calibration of simulation models that can consider C allocation

schemes in forests (e.g., LANDIS-II with CENTURY extension [Scheller et al. 2011*a*, *b*]; LPJ [Sitch et al. 2003]; IBIS [Kucharik et al. 2000]). Our study addresses that need for Rocky Mountain subalpine forests at a landscape scale. Yet, we found that TBCF partitioning can vary geographically within even the same forest type. Allowing C flux partitioning to respond to variability in forest structure and soil fertility would help improve predictions of forest C cycling responses to changing climate, disturbance regimes, and management scenarios. Because the size of the forest C sink results from the difference between two enormous fluxes, even a change as small as a few percent, as seen here, may have a large impact on the C balance of the forest.

In spite of increased understanding of controls over soil respiration and TBCF, estimating belowground C fluxes over large spatial extents remains challenging. Current global NPP data products rely on lookup tables of respiration that are only specific at the biome level (Running et al. 2004). Our findings illustrate that forest C cycling depends on forest structure, which is often determined by disturbance history, and soil fertility. Forest height can be obtained for large areas from national forest inventories (e.g., USFS FIA Program) or light detection and ranging technologies (lidar; Lefsky 2010). Leaf area index can also be quantified across large regions using remotely sensed data and imagery from fine- and moderate-resolution satellites (e.g., MODIS or Landsat; Myneni et al. 2002, Cohen et al. 2003). There is also potential to use remotely sensed disturbance history to project forest structure across the landscape (Huang et al. 2010). In contrast to aboveground forest properties, accurate spatial data on soil N are more difficult to obtain. For example, soil sampling is included as standard FIA protocol in the United States; however, because the plots with soil sampling are sparsely distributed (one per 388 km^2), a spatially explicit soil N product would have a spatial resolution that would be too low for use at the forest type level. Soil N is estimated in global and national databases, but sampling is spatially inconsistent and the data often have coarse spatial resolution compared to forest data; gaps in soil data are also common in mountainous regions (e.g., SSURGO and WISE [Batjes 2014]). Reducing uncertainty and increasing the spatial resolution of soil N maps would aid efforts to accurately estimate TBCF patterns across large landscapes.

For purposes of constructing regional C cycle budgets, consider the accuracy gained by leveraging existing information about forest ecosystem properties. Across all three sites, we found a mean TBCF of 4.89 $Mg{\cdot}C{\cdot}ha^{-1}{\cdot}yr^{-1}$. The estimated uncertainty (RMSE) of this value represents 17% of the mean TBCF (Table 2). However, we incorporated additional information about LAI and soil N on the landscape and reduced this uncertainty to 11% of the mean TBCF (Table 2). This difference, 304 kg of $C{\cdot}ha^{-1}{\cdot}yr^{-1}$, is roughly equivalent to one-fourth of the net ecosystem carbon balance of these three sites (Bradford et al. 2008)—a significant amount of C. This reduction in uncertainty enabled by forest and soil data is a clear advantage for characterizing regional forest C budgets.

Acknowledgments

The USFS North American Carbon Program and the USGS Climate and Land Use Change Mission Area funded this work. Data collection was funded by NASA grant CARBON/04-0225-0191. Any use of trade, product, or firm names is for descriptive purposes only and does not imply endorsement by the U.S. Government. The authors acknowledge the efforts of Brianna Miles for data collection, as well as Jennifer Briggs (USGS) and anonymous peer reviewers whose comments greatly improved the quality of this manuscript.

Literature Cited

Ambrose, A. R., S. C. Sillett, and T. E. Dawson. 2009. Effects of tree height on branch hydraulics, leaf structure and gas exchange in California redwoods. Plant, Cell & Environment 32:743–757.

Argerich, A., S. L. Johnson, S. D. Sebestyen, C. C. Rhoades, E. Greathouse, J. D. Knoepp, M. B. Adams, G. E. Likens, J. L. Campbell, and W. H. McDowell. 2013. Trends in stream nitrogen concentrations for forested reference catchments across the USA. Environmental Research Letters 8:014039.

Barnard, H. R., and M. G. Ryan. 2003. A test of the hydraulic limitation hypothesis in fast-growing *Eucalyptus saligna*. Plant, Cell & Environment 26: 1235–1245.

Batjes, N. H. 2014. Total carbon and nitrogen in the soils of the world. European Journal of Soil Science 65:10–21.

Bechtold, W. A., and P. L. Patterson. 2005. The enhanced forest inventory and analysis program: national sampling design and estimation procedures. USDA Forest Service, Southern Research Station, Asheville, North Carolina, USA.

Beets, P. N., and D. Whitehead. 1996. Carbon partitioning in *Pinus radiata* stands in relation to foliage nitrogen status. Tree Physiology 16:131–138.

Berg, B., and E. Matzner. 1997. Effect of N deposition on decomposition of plant litter and soil organic matter in forest systems. Environmental Reviews 5:1–2.

Binkley, D., J. L. Stape, and M. G. Ryan. 2004. Thinking about efficiency of resource use in forests. Forest Ecology and Management 193:5–16.

Bond-Lamberty, B., C. Wang, and S. T. Gower. 2002. Aboveground and belowground biomass and sapwood area allometric equations for six boreal tree species of northern Manitoba. Canadian Journal of Forest Research 32:1441–1450.

Bradford, J. B., R. A. Birdsey, L. A. Joyce, and M. G. Ryan. 2008. Tree age, disturbance history, and carbon stocks and fluxes in subalpine Rocky Mountain forests. Global Change Biology 14:2882–2897.

Bradford, J. B., P. Weishampel, M.-L. Smith, R. Kolka, R. A. Birdsey, S. V. Ollinger, and M. G. Ryan. 2010. Carbon pools and fluxes in small temperate forest landscapes: variability and implications for sampling design. Forest Ecology and Management 259:1245–1254.

Cohen, W. B., T. K. Maiersperger, Z. Yang, S. T. Gower, D. P. Turner, W. D. Ritts, M. Berterretche, and S. W. Running. 2003. Comparisons of land cover and LAI estimates derived from ETM+ and MODIS for four sites in North America: a quality assessment of 2000/2001 provisional MODIS products. Remote Sensing of Environment 88:233–55. http://dx.doi.org/10.1016/j.rse.2003.06.006

Comeau, P. G., and J. P. Kimmins. 1989. Above- and below-ground biomass and production of lodgepole pine on sites with differing soil moisture regimes. Canadian Journal of Forest Research 19:447–454.

Davidson, E. A., A. D. Richardson, K. E. Savage, and D. Y. Hollinger. 2006. A distinct seasonal pattern of the ratio of soil respiration to total ecosystem respiration in a spruce-dominated forest. Global Change Biology 12:230–239.

Drake, J. E., L. M. Raetz, S. C. Davis, and E. H. DeLucia. 2010. Hydraulic limitation not declining nitrogen availability causes the age-related photosynthetic decline in loblolly pine (*Pinus taeda* L.). Plant, Cell & Environment 33:1756–1766.

Duursma, R. A., J. D. Marshall, and A. P. Robinson. 2003. Leaf area index inferred from solar beam transmission in mixed conifer forests on complex terrain. Agricultural and Forest Meteorology 118:221–236.

Entekhabi, D., et al. 2010. The soil moisture active passive (SMAP) mission. Proceedings of the IEEE 98:704–716.

Forrester, D. I., J. Bauhus, and A. L. Cowie. 2006. Carbon allocation in a mixed-species plantation of *Eucalyptus globulus* and *Acacia mearnsii*. Forest Ecology and Management 233:275–284.

Franklin, O., J. Johansson, R. C. Dewar, U. Dieckmann, R. E. McMurtrie, Å. Brännström, and R. Dybzinski. 2012. Modeling carbon allocation in trees: a search for principles. Tree Physiology 32:648–666.

Giardina, C. P., and M. G. Ryan. 2002. Total belowground carbon allocation in a fast-growing *Eucalyptus* plantation estimated using a carbon balance approach. Ecosystems 5:487–499.

Giardina, C. P., M. G. Ryan, D. Binkley, and J. H. Fownes. 2003. Primary production and carbon allocation in relation to nutrient supply in a tropical experimental forest. Global Change Biology 9:1438–1450.

Giardina, C. P., D. Binkley, M. G. Ryan, J. H. Fownes, and R. S. Senock. 2004. Belowground carbon cycling in a humid tropical forest decreases with fertilization. Oecologia 139:545–550.

Giardina, C. P., M. D. Coleman, J. E. Hancock, J. S. King, E. A. Lilleskov, W. M. Loya, K. S. Pregitzer, M. G. Ryan, and C. C. Trettin. 2005. The response of belowground carbon allocation in forests to global change. Pages 119–154 *in* O. Menyailo and D. Binkley, editors. Tree species effects on soils: implications for global change. Kluwer, Dordrecht, The Netherlands.

Giardina, C. P., C. M. Litton, S. E. Crow, and G. P. Asner. 2014. Warming-related increases in soil CO_2 efflux are explained by increased below-ground carbon flux. Nature Climate Change 4:822–827.

Heath, L. S., J. E. Smith, K. E. Skog, D. J. Nowak, and C. W. Woodall. 2011. Managed forest carbon estimates for the US greenhouse gas inventory, 1990-2008. Journal of Forestry 109:167–173.

Huang, C., et al. 2010. An automated approach for reconstructing recent forest disturbance history using dense Landsat time series stacks. Remote Sensing of Environment 114:183–198.

Hubbard, R. M., M. G. Ryan, K. Elder, and C. C. Rhoades. 2005. Seasonal patterns in soil surface CO_2 flux under snow cover in 50 and 300 year old subalpine forests. Biogeochemistry 73:93–107.

Janssens, I. A., W. Dieleman, S. Luyssaert, J.-A. Subke, M. Reichstein, R. Ceulemans, P. Ciais, A. J. Dolman, J. Grace, and G. Matteucci. 2010. Reduction of forest soil respiration in response to nitrogen deposition. Nature Geoscience 3:315–322.

Kaufmann, M. R., C. B. Edminster, and C. A. Troendle. 1982. Leaf area determinations for subalpine tree species in the central Rocky Mountains. Rocky Mountain Forest and Range Experiment Station, Fort Collins, Colorado, USA.

Keith, H., R. J. Raison, and K. L. Jacobsen. 1997. Allocation of carbon in a mature eucalypt forest and some effects of soil phosphorus availability. Plant and Soil 196:81–99.

Ker, M. F., and G. D. V. Raalte. 1981. Tree biomass equations for *Abies balsamea* and *Picea glauca* in northwestern New Brunswick. Canadian Journal of Forest Research 11:13–17.

King, A. W., R. J. Andres, K. J. Davis, M. Hafer, D. J. Hayes, D. N. Huntzinger, B. de Jong, W. A. Kurz, A. D. McGuire, and R. Vargas. 2015. North America's net terrestrial CO_2 exchange with the atmosphere 1990-2009. Biogeosciences 12:399–414.

Kucharik, C. J., J. A. Foley, C. Delire, V. A. Fisher, M. T. Coe, J. D. Lenters, C. Young-Molling, N. Ramankutty, J. M. Norman, and S. T. Gower. 2000. Testing the performance of a dynamic global ecosystem model: water balance, carbon balance, and vegetation structure. Global Biogeochemical Cycles 14:795–825.

Lefsky, M. A. 2010. A global forest canopy height map from the Moderate Resolution Imaging Spectroradiometer and the Geoscience Laser Altimeter System. Geophysical Research Letters 37:L15401.

Litton, C. M., M. G. Ryan, and D. H. Knight. 2004. Effects of tree density and stand age on carbon allocation patterns in postfire lodgepole pine. Ecological Applications 14:460–475.

Litton, C. M., J. W. Raich, and M. G. Ryan. 2007. Carbon allocation in forest ecosystems. Global Change Biology 13:2089–2109.

Ma, W. L., P. L. Shi, W. H. Li, Y. T. He, X. Z. Zhang, Z. X. Shen, and S. Y. Chai. 2010. Changes in individual plant traits and biomass allocation in alpine meadow with elevation variation on the Qinghai-Tibetan Plateau. Science China-Life Sciences 53:1142–1151.

Maier, C. A., T. J. Albaugh, H. L. Allen, and P. M. Dougherty. 2004. Respiratory carbon use and carbon storage in mid-rotation loblolly pine (*Pinus taeda* L.) plantations: the effect of site resources on the stand carbon balance. Global Change Biology 10:1335–1350.

Massman, W. J. 1998. A review of the molecular diffusivities of H_2O, CO_2, CH_4, CO, O_3, SO_2, NH_3, N_2O, NO, and NO_2 in air, O_2 and N_2 near STP. Atmospheric Environment 32:1111–1127.

McCarthy, H. R., R. Oren, A. C. Finzi, and K. H. Johnsen. 2006. Canopy leaf area constrains $[CO_2]$-induced enhancement of productivity and partitioning among aboveground carbon pools. Proceedings of the National Academy of Sciences USA 103:19356–19361.

Myers, C. A. 1964. Volume tables and point-sampling factors for lodgepole pine in Colorado and Wyoming. Research Paper RM 6. Rocky Mountain Forest and Range Experiment Station, Fort Collins, Colorado, USA.

Myers, C. A. 1972. Volume tables and point sampling factors for Engelmann spruce in Colorado and Wyoming. Research Paper RM 95. Rocky Mountain Forest and Range Experiment Station, Fort Collins, Colorado, USA.

Myneni, R. B., S. Hoffman, Y. Knyazikhin, J. L. Privette, J. Glassy, Y. Tian, Y. Wang, X. Song, Y. Zhang, and G. R. Smith. 2002. Global products of vegetation leaf area and fraction absorbed PAR from year one of MODIS data. Remote Sensing of Environment 83:214–231.

National Atmospheric Deposition Program. 2015. NTN data retrieval options. Illinois State Water Survey, Champaign, Illinois, USA. National Atmospheric Deposition Program office. http://nadp.isws.illinois.edu/NTN/ntnData.aspx

Nave, L. E., C. W. Swanston, U. Mishra, and K. J. Nadelhoffer. 2013. Afforestation effects on soil carbon storage in the United States: a synthesis. Soil Science Society of America Journal 77:1035–1047.

Olsson, U., D. Binkley, and F. W. Smith. 1997. Nitrogen supply, nitrogen use, and production in an age sequence of lodgepole pine. Forest Science 44:454–457.

Olsson, P., S. Linder, R. Giesler, and P. Högberg. 2005. Fertilization of boreal forest reduces both autotrophic and heterotrophic soil respiration. Global Change Biology 11:1745–1753.

Palmroth, S., R. Oren, H. R. McCarthy, K. H. Johnsen, A. C. Finzi, J. R. Butnor, M. G. Ryan, and W. H. Schlesinger. 2006. Aboveground sink strength in forests controls the allocation of carbon below ground and its $[CO_2]$-induced enhancement. Proceedings of the National Academy of Sciences USA 103:19362–19367.

R Core Team. 2016. R: a language and environment for statistical computing. R Foundation for Statistical Computing, Vienna, Austria. https://www.R-project.org/

Raich, J. W. 1998. Aboveground productivity and soil respiration in three Hawaiian rain forests. Forest Ecology and Management 107:309–318.

Raich, J. W., and K. J. Nadelhoffer. 1989. Belowground carbon allocation in forest ecosystems: global trends. Ecology 70:1346–1354.

Rollins, M. G. 2009. LANDFIRE: a nationally consistent vegetation, wildland fire, and fuel assessment. International Journal of Wildland Fire 18:235–249.

Ruark, G. A., and J. G. Bockheim. 1988. Biomass, net primary production, and nutrient distribution for

an age sequence of *Populus-tremuloides* ecosystems. Canadian Journal of Forest Research 18:435–443.

Running, S. W., R. R. Nemani, F. A. Heinsch, M. Zhao, M. Reeves, and H. Hashimoto. 2004. A continuous satellite-derived measure of global terrestrial primary production. BioScience 54:547–560.

Ryan, M. G. 1995. Foliar maintenance respiration of subalpine and boreal trees and shrubs in relation to nitrogen content. Plant, Cell & Environment 18:765–772.

Ryan, M. G., and R. H. Waring. 1992. Maintenance respiration and stand development in a subalpine lodgepole pine forest. Ecology 73:2100–2108.

Ryan, M. G., and B. J. Yoder. 1997. Hydraulic limits to tree height and tree growth. BioScience 47:235–242.

Ryan, M. G., D. Binkley, J. H. Fownes, C. P. Giardina, and R. S. Senock. 2004. An experimental test of the causes of forest growth decline with stand age. Ecological Monographs 74:393–414.

Ryan, M. G., N. Phillips, and B. J. Bond. 2006. The hydraulic limitation hypothesis revisited. Plant, Cell & Environment 29:367–381.

Scheller, R. M., D. Hua, P. V. Bolstad, R. A. Birdsey, and D. J. Mladenoff. 2011*a*. The effects of forest harvest intensity in combination with wind disturbance on carbon dynamics in Lake States Mesic Forests. Ecological Modelling 222:144–153.

Scheller, R. M., S. Van Tuyl, K. L. Clark, J. Hom, and I. La Puma. 2011*b*. Carbon sequestration in the New Jersey pine barrens under different scenarios of fire management. Ecosystems 14:987–1004.

Sitch, S., B. Smith, I. C. Prentice, A. Arneth, A. Bondeau, W. Cramer, J. O. Kaplan, S. Levis, W. Lucht, and M. T. Sykes. 2003. Evaluation of ecosystem dynamics, plant geography and terrestrial carbon cycling in the LPJ dynamic global vegetation model. Global Change Biology 9:161–185.

Smith, F. W., and S. C. Resh. 1999. Age-related changes in production and below-ground carbon allocation in *Pinus contorta* forests. Forest Science 45: 333–341.

Smithwick, E. A., D. M. Kashian, M. G. Ryan, and M. G. Turner. 2009. Long-term nitrogen storage and soil nitrogen availability in post-fire lodgepole pine ecosystems. Ecosystems 12:792–806.

Speckman, H. N., J. M. Frank, J. B. Bradford, B. L. Miles, W. J. Massman, W. J. Parton, and M. G. Ryan. 2015. Forest ecosystem respiration estimated from eddy covariance and chamber measurements under high turbulence and substantial tree mortality from bark beetles. Global Change Biology 21:708–721.

Stape, J. L., D. Binkley, and M. G. Ryan. 2008. Production and carbon allocation in a clonal *Eucalyptus* plantation with water and nutrient manipulations. Forest Ecology and Management 255:920–930.

Wang, J. R., A. L. Zhong, P. Comeau, M. Tsze, and J. P. Kimmins. 1995. Aboveground biomass and nutrient accumulation in an age sequence of aspen (*Populus tremuloides*) stands in the boreal white and black spruce zone, British Columbia. Forest Ecology and Management 78:127–138.

Woodbury, P. B., J. E. Smith, and L. S. Heath. 2007. Carbon sequestration in the US forest sector from 1990 to 2010. Forest Ecology and Management 241:14–27.